

Optical properties of copper in silicon: Excitons bound to isoelectronic copper pairs

J. Weber, H. Bauch, and R. Sauer

*Physikalisches Institut (Teil 4) der Universität Stuttgart, Pfaffenwaldring 57,
D-7000 Stuttgart 80, Federal Republic of Germany*

(Received 9 February 1982)

Copper doping of silicon crystals results in an intense emission at 1.014 eV. The photoluminescence spectrum exhibits a characteristic structure consisting of a narrow no-phonon line and equispaced lower-energy resonant-mode phonon replicas. The typical phonon energy is 7.0 meV. We observe isotope shifts of the lines which conclusively show that copper is incorporated in the luminescent defect. Combination with the observed quadratic dependence of the emission intensity on copper concentration leads us to suggest copper pairs as recombination centers. The symmetry of the pair as determined from uniaxial stress and Zeeman data is that of a $\langle 111 \rangle$ configuration. The no-phonon line structure and the splitting in external fields indicate an exciton localized at an isoelectronic trap. The exciton is discussed in terms of an isoelectronic donor combining the present data with recent deep-level transient-spectroscopy results.

I. INTRODUCTION

Deep impurities which introduce energy levels near the middle of the forbidden gap drastically influence the electrical conductivity and the free-carrier lifetime of semiconductors. In silicon, the transition metals belong to this group of deep impurities. Among all transition metals, copper has an unusually large diffusion coefficient and a high solid solubility at high temperatures. These properties are attributed to the fact that copper mainly occupies interstitial lattice sites in silicon. They make copper a feared contaminant in all technological processes which imply heating of the material. A large fraction of the copper atoms introduced form precipitates after diffusion and cooling since the solubility of copper is at room temperature reduced by several orders of magnitude. Precipitation occurs preferentially at stacking faults and serves to decorate such lattice defects.

Values of the solid solubility of copper in silicon were determined by several authors^{1,2} and were summarized by Trumbore.³ Hall and Racette⁴ in a later work confirmed the former results. All authors applied the tracer method using radioactive ⁶⁴Cu. The measurements yielded an absolute copper concentration of about $5 \times 10^{16} \text{ cm}^{-3}$ at 800°C. The solubility reaches a saturation value of about 10^{18} cm^{-3} at 1300°C. In Hall measurements,² however, a substantially smaller maximum concentration ($\sim 10^{14} \text{ cm}^{-3}$) of electrically active

centers was observed. Recent deep-level transient-spectroscopy (DLTS) data by Graff and Pieper⁵ confirmed these comparatively low concentration values. These authors suggested that the concentration of electrically active copper centers is mainly determined by the sample preparation, in particular by the cooling rate of the samples after diffusion. They found a maximum concentration of 10^{14} cm^{-3} active centers at 800°C, and a decrease of concentrations at higher diffusion temperatures. The difference between the absolute copper concentrations as determined by the tracer method and the concentrations of electrically active copper centers is generally attributed to the precipitation of copper atoms.

A typical property of all deep impurities is their ability to form complexes with other impurities. Such a tendency was supposed to be also important for copper in silicon. Hall and Racette⁴ assumed from conductivity measurements a pairing of substitutional copper atoms with shallow donors. Ludwig and Woodbury⁶ briefly reported EPR measurements on defects involving pairs of copper with the deep impurities chromium, manganese, or iron. Although EPR studies were successfully performed on almost all isolated transition-metal elements in silicon yielding their position in the lattice and their ground-state symmetry, similar studies were ineffectual in the case of copper.

Up to now, only few photoluminescence investigations of deep centers in silicon exist. A recent

luminescence study on iron-doped silicon demonstrated that this transition metal gives rise to a variety of emission lines in the wavelength range from 1.2 to 1.7 μm .⁷ A number of other emission lines are ascribed to pairs of iron and shallow acceptors, e.g., Fe-In,⁸ Fe-B, and to Cr-B.⁹ It was very recently suggested¹⁰ that new emission features observed in gold-doped silicon are due to the gold impurity. However, the question seems to be open whether this emission is directly correlated with gold or with some other contaminant unintentionally introduced during the gold diffusion. Contrary to the case of silicon, the photoluminescence due to transition metals was widely and intensely investigated in the III-V and the II-VI compound semiconductors. Copper particularly induces in most host crystals strong luminescence lines.¹¹ The luminescent centers often have a symmetry lower than cubic expressing the fact that copper forms associates with other defects.

The present paper reports on luminescence spectra from copper-doped silicon. In Sec. II, we describe the general features of the emission spectra. Section III is devoted to an elucidation of the defect's chemical nature as a copper pair by sample preparation and isotope doping. In Sec. IV, we derive the electronic level scheme of the copper complex. The splitting of the emission lines in uniaxial stress fields and in magnetic fields is discussed in Secs. V and VI, respectively. Finally, Sec. VII presents a discussion of the results.

The experiments were performed with the samples immersed in liquid helium which could be pumped if necessary. For the temperature-controlled measurements, we used a special cryostat operating from 4 to about 100 K at relatively high permissible excitation powers (see Ref. 12). The luminescence was excited by a cw argon-ion or a krypton-ion laser (514 or 647 nm, respectively) at powers up to 1.5 W, and dispersed with a Spex monochromator of 1-m focal length. The signals were detected by a germanium detector (North Coast) and processed by conventional lock-in technique (Ithaco, Dynatrac). Magnetic fields up to 5.3 T were generated by a superconducting cryomagnet in a split-coil configuration. Uniaxial stress measurements were performed in the conventional technique with the samples cut into parallelepipeds (approximately $2 \times 2 \times 8 \text{ mm}^3$) and put between two stainless-steel pistons in the helium bath (long edge parallel to stress axis). Stress was applied by adjusted springs or via a system of lever arms and weights outside the Dewar.

II. GENERAL FEATURES OF THE COPPER-INDUCED LUMINESCENCE

Copper-doped silicon crystals exhibit at low temperatures a characteristic emission spectrum at an energy well below the familiar near-band-gap extrinsic luminescence from group-III acceptor or group-V donor-bound excitons (Fig. 1). The spectrum is made up of a narrow no-phonon (NP) line Cu_0^0 which is replicated at lower energies by successively broader and weaker satellites, Cu_0^1 , etc. This sharp line structure is superimposed on a broad band centered at about 0.95 eV. All lines are due to *one* defect; first since the same spectrum is seen in all samples independent of the preceding preparation procedure and second since all lines split identically when uniaxial stress is applied and exhibit the same temperature dependence in the optical experiment. The positions of the more intense lines and their halfwidths are summarized in Table I. The weaker lines are not included in Table I. They are displaced from each other by about 7 meV as are the tabulated lines. The properties of the satellites identify them as phonon replicas of the principle NP line. The phonons are not momentum conserving as in familiar near-band-gap luminescence¹² but are in-band resonant modes associated with local vibrations of the luminescent center. Similar resonant phonon modes have been

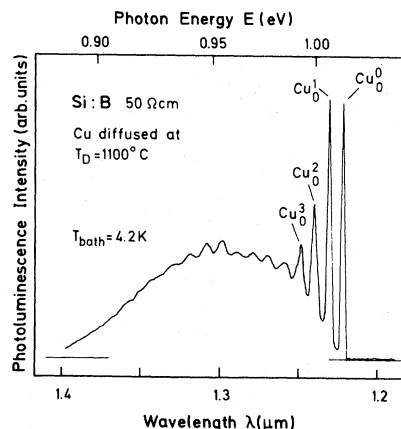


FIG. 1. Photoluminescence spectrum of Cu-doped silicon at 4.2-K bath temperature. Cu_0^0 is the no-phonon (NP) transition. The lower-energy replicas (Cu_0^1 , etc.) are due to the excitation of resonant-mode phonons in the optical transition (characteristic phonon energy 7.0 meV). The upper labeling index of the lines denotes the number of excited phonons. The lower index characterizes the upper electronic ground state.

TABLE I. Labeling and spectroscopic parameters of the copper-induced photoluminescence lines.

Line	Transition	λ (μm)	$h\nu$ (eV)	Displacement from Cu_0^0 (meV)	Halfwidth (meV)	Remarks
Cu_0^0	no-phonon	1.2217	1.0145 ₅		0.14	
Cu_0^1	Stokes	1.2302	1.0075 ₅	-7.0	0.62	Helium temperature ($T \approx 4$ K)
Cu_0^2		1.2389	1.0005	-14.0	1.1	
Cu_0^3		1.2478	0.9933	-21.2	2.2	
Cu_0^{-1}	anti-Stokes	1.2134	1.0215	+7.0	2.0	Higher temperature
Cu_0^{-2}		1.2054	1.0283	+13.7	2.6	
Cu_1^0	no-phonon excited	1.2195	1.0164	+1.9	0.8	(T \approx 30 K)
Cu_2^0		1.2103	1.0241	+9.6	0.8	

found in the luminescence of iron-doped silicon⁷ and in the spectrum of the isoelectronic *P, Q, R* lines which appear in indium-doped silicon¹³ and were attributed to Fe-In pairs.⁸ The phonon energy is in each case typical of the transition-metal elements apart from some slight variations due to perturbations by the associate defect partners. As an example, we note that Fe couples to phonons of 9.5-meV energy⁷ and Cr seems to couple to 13.5-meV phonons.⁹

A photoluminescence spectrum as in Fig. 1 was already similarly observed by Minaev *et al.*¹⁴ from samples which were thermally treated but were not intentionally doped with copper. These authors heated Czochralski- (CZ) grown silicon to 1300°C for a short time and cooled the samples rapidly by dropping them into water or oil at room temperature. They studied the dependence of the line intensities on diffusion temperatures and found that the lines anneal out when the samples are heated to moderately high temperatures. In that work, attempts were made to determine the symmetry of the defect. Unfortunately, the splitting patterns shown are at variance with the text, and a repetition of the symmetry determination seemed to be highly desirable. Minaev *et al.* called the luminescent center a "thermal defect" in view of the technique of generating the radiation, and supposed that some transition metal was responsible for the emission without going into detailed experimental studies to clarify this point.

III. CHEMICAL NATURE OF THE TRAP

Doping of the samples was performed by the diffusion of copper films which were evaporated on both sides of silicon slices. The slices were about 0.5 mm thick, but in special cases the thickness was up to 3 mm, e.g., when uniaxial stress should be applied. The diffusion was performed for 5 min in a vertical furnace from which the samples were directly dropped into an oil bath at room temperature. It turned out that a high cooling rate was favorable for obtaining strong emission. Heating times longer than 5 min did not noticeably influence the emission. The samples were then mechanically lapped and etched in a mixture of HF and HNO₃ (1:3) and stored in liquid nitrogen.

It is possible that during this procedure some contamination was introduced which might be the origin of the emission heretofore ascribed to copper. To clearly identify copper as responsible for the radiation, we implanted ⁶³Cu or ⁶⁵Cu isotopes, respectively, in two high-resistivity float zone (FZ) silicon samples. The implanted specimens were then diffused and quenched as described above. Both specimens exhibited spectra quite similar to that in Fig. 1 but the position of the NP line was shifted by ~ -0.02 meV for ⁶³Cu-doped silicon, and by $\sim +0.04$ meV for ⁶⁵Cu-doped silicon (Fig. 2). Likewise, shifts of the phonon satellites were observed which are discussed below. It

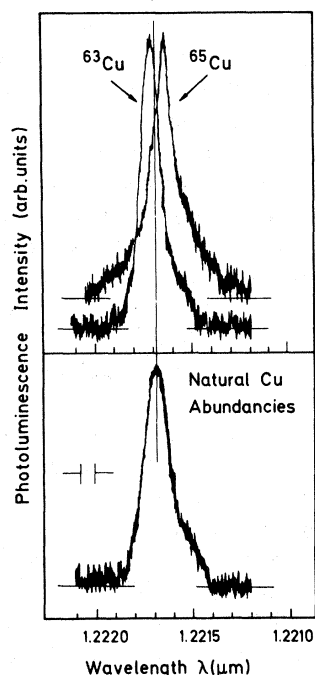


FIG. 2. Upper part denotes spectral positions of the Cu_0^0 line in silicon doped with either ^{63}Cu or ^{65}Cu isotopes. Lower part denotes spectrum of the Cu_0^0 line in silicon containing Cu in natural isotope abundances. The unresolved line on the high-energy shoulder is split apart by about 0.15 meV and is discussed in the text.

is striking that the lines from samples containing copper in natural isotope abundances ($^{65}\text{Cu}:[^{63}\text{Cu}]$ as 1:2.2) are distinctly broader than those from ^{63}Cu - or ^{65}Cu -doped ones suggesting that the former line is an appropriate superposition of the single-isotope lines. All lines when observed in high resolution are unsymmetric showing high-energy shoulders which become more prominent upon a temperature increase. This property hints to an excited state approximately 0.15 meV above the upper ground state of the NP optical transition. The excited state will be verified and discussed further in Sec. VI.

These measurements give evidence that the observed luminescence is related to copper. Isotope shifts of luminescence lines are a common feature of deep centers and have often been a convenient tool in identifying the chemical nature of such centers. Heine and Henry¹⁵ gave a quantitative theory of isotope shifts of NP optical transitions associated with the decay of excitons bound to deep traps. NP lines are transitions between electronic states with no phonons participating either in the initial or in the final state. Either state,

however, has zero-point vibrational energy. If the force constant in the initial electronic state is different from the one in the final state, an isotope splitting of the NP optical transition will result. Experimentally, the heavier isotope is normally found to produce the higher-energy line. van Vechten¹⁶ on the basis of the above-mentioned theory gave an explanation of some peculiar cases showing inverse isotope effects.

The simple model of the trap being in an approximately harmonic vibrational potential as used by Heine and Henry also predicts isotope splittings of the phonon satellites. We have in fact observed that the first satellite Cu_0^1 was differently displaced from its associated NP isotope line by $\Delta E(^{63}\text{Cu}) \approx 7.03$ meV and $\Delta E(^{65}\text{Cu}) \approx 6.96$ meV. Isotope-dependent shifts of the next satellites could not be measured due to the large half-widths. For the Cu_0^1 phonon lines, the ratio of the displacement energies is 1.010, close to the value of $(\frac{65}{63})^{1/2} = 1.0157$ which results from the simple model when the same force constant for both Cu isotopes is assumed in the electronic ground state.

The luminescence intensity of the copper-induced lines depends strongly on the diffusion temperature and on the quenching rate. In our sample preparation technique, we kept the quenching rate fixed and as high as possible after some initial variation to optimize the luminescence and varied the diffusion temperature systematically. At a diffusion temperature of 700°C, the Cu luminescence as well as the familiar near-band-gap lines show up. When the diffusion temperature is increased to 900°C and above, the Cu luminescence strongly increases, and the near-band-gap lines disappear. The characteristic structure of the Cu spectrum and the line positions are not altered in this process. Figure 3 depicts the dependence of the NP line intensity on the diffusion temperature. This logarithmic plot against the reciprocal temperature yields a straight line up to temperatures of about 1100°C. We believe that the intensity increase is due to the higher solid solubility of copper at higher temperatures. Since the diffusion constant of copper is high, we always reach—at diffusion times of 5 min and a sample thickness on order of 1 mm—the maximum copper concentration given by the actual solubility value. Our copper concentrations are determined from a comparison with data by Struthers.¹ The correlation of the copper concentration N_{Cu} with the diffusion temperature which Struthers finds is shown in Fig. 3 by the double-valued abscissa with a temperature

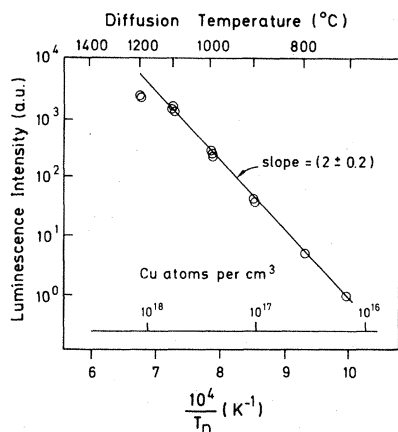


FIG. 3. Luminescence intensity of the Cu_0^0 line as a function of diffusion temperature. The double-valued abscissa gives the copper concentration as a function of diffusion temperature after Struthers (Ref. 1).

scale identical to the one of our present luminescence measurements. Considering the intensity-versus-concentration dependence which results from the double logarithmic plot in Fig. 3, we find a quadratic dependence of the intensity I on the copper concentration N_{Cu} ,

$$I \propto N_{\text{Cu}}^{(2 \pm 0.2)}.$$

The intensity value at 1200°C is in Fig. 3 below the value expected from this expression. This may be due to the precipitation of copper at higher concentrations or to saturation effects of the solid solubility.

We interpret the above expression $I(N_{\text{Cu}})$ in terms of second-order reaction kinetics assuming that the luminescence intensity is proportional to the concentration of the trap. Consequently, we conclude that two copper atoms are incorporated in the luminescent trap. This leaves open the possibility that further partners other than copper are involved.

In all our experiments we could not find any dependence of the copper-induced spectrum on the donor or acceptor doping of the starting material. This refers to the doping species of phosphorous, boron, and aluminum, and to concentrations from 10^{12} up to 10^{17} cm^{-3} . Only at high concentrations ($> 10^{17} \text{ cm}^{-3}$) the intensity of the copper spectrum decreased. Combining these latter results with the former copper concentration dependence, we find some probability that copper pairs alone constitute the luminescent trap. We note that the pair model is consistent with, although not confirmed by, a

line-shape fit since the natural abundance spectrum can be obtained from the two pure isotope spectra by assuming that *either* one or two copper atoms are involved in the complex.

The center shows a complex behavior under isochronal (30 min) annealing conditions (Fig. 4). At 150°C, the intensity has a maximum. Above 300°C, the luminescence signal has completely vanished, and does not reappear upon room-temperature annealing within three days. The center can be easily reactivated by heating the samples again to higher temperatures and quenching them subsequently in oil.

No absorption of the samples due to copper could be detected although the luminescence intensities are quite high compared to other emission lines in silicon. Instead, when the absorption experiments were performed as described elsewhere,¹² we observed luminescence. This situation is reminiscent of the *A, B, C* emission lines¹² and of the *P, Q, R* luminescence system^{8,13} in silicon which could also never be observed in absorption. In these cases, it was suggested that the luminescence is due to the decay of excitons localized at isoelectronic traps. Therefore, from our negative absorption result we may suppose a high radiative quantum efficiency of the copper luminescence which hints also in the present case to an isoelectronic binding trap.

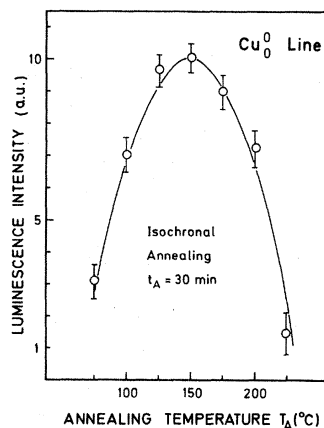


FIG. 4. Luminescence intensity of the Cu_0^0 line after isochronal annealing (annealing time $t_A = 30 \text{ min}$). The starting material was boron-doped silicon ($10 \Omega \text{ cm}$) which was copper diffused at 1000°C.

IV. ELECTRONIC LEVEL SCHEME OF THE LOCALIZED EXCITON

Temperature-dependent luminescence measurements were performed to determine the electronic level scheme of the exciton bound to the copper trap. The temperature could be varied between 4.2 and 100 K. In Fig. 5, we compare two spectra recorded at temperatures of 5 or 30 K, respectively. The lower spectrum corresponds to the one of Fig. 1 except for higher resolution. In the upper spectrum, the intensity of all lines has largely dropped, only the broad underlying band with maximum at about $1.3 \mu\text{m}$ (0.95 eV) has increased. This band alone persists at temperatures above 80 K. The local-mode satellites are broader than at lower temperature. New lines arise on the high-energy side of the NP line. The lines Cu_0^{-1} and Cu_0^{-2} are of comparable width to the low-energy phonon satellites; the lines Cu_1^0 and Cu_2^0 are much narrower (cf. Table I). The lines Cu_0^{-1} and Cu_0^{-2} are displaced from the NP line by +7.0 meV or +13.7 meV, respectively, and grow relative to Cu_0^0 upon further temperature increase. The spectra are consistent with equal activation energies to the spectroscopic displacements although an accurate determination was not made with regard to the weakness and the broad, temperature-dependent halfwidths of the lines. They are evidently anti-Stokes phonon satellites annihilating one or two resonant phonons in the event of the optical transition. The remaining lines Cu_1^0 and Cu_2^0 are identified as no-phonon transitions on the basis of their sharpness. They thermalize with the NP (Cu_0^0) line with activation energies close to their spectroscopic displacements from that line which are $E_1 = 1.9$ meV or $E_2 = 9.6$ meV, respectively. Therefore, we

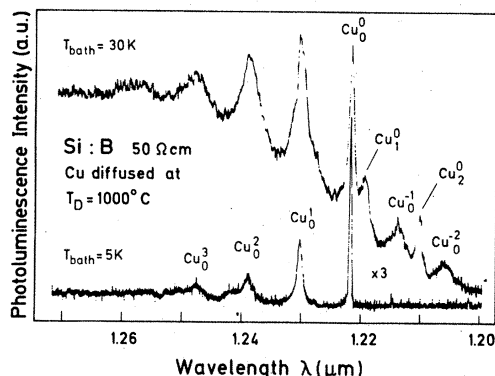


FIG. 5. High-resolution luminescence spectra of the Cu emission at bath temperatures of 5 and 30 K. For the line positions and halfwidths, see Table I.

attribute them to excitations of the upper electronic states of the trap. The analysis of the temperature-dependent intensity ratios yields the following degeneracies from an extrapolation to infinite temperature:

$$\frac{g(\text{Cu}_1^0)}{g(\text{Cu}_0^0)} = 0.5 \pm 0.1$$

and

$$\frac{g(\text{Cu}_2^0)}{g(\text{Cu}_0^0)} = 1.0 \pm 0.1.$$

Absolute temperature-dependent intensities I of the principle NP line Cu_0^0 are plotted in Fig. 6 in a logarithmic scale against the reciprocal temperature. The experimental points were fitted using the expression for $I(T)$ as inserted in Fig. 6. This expression results on the assumption that the total number of excitons which are regarded is constant and does not depend on temperature, and that the relative population of the different exciton states is thermal.^{17,18} The formula which we apply in Fig. 6 assumes four levels, the transition upper ground state at E_0 and excited states at excess energies of E_1 , E_2 , and E_3 . The fit in Fig. 6 was performed according to a least-squares criterion. We find the values $E_1 = 1.9$ meV, $E_2 = 9.6$ meV, and $E_3 = 32$ meV. The former two values are identical with the spectroscopic spacings between the line pairs Cu_0^0 and Cu_1^0 or Cu_0^0 and Cu_2^0 , respectively. The factor

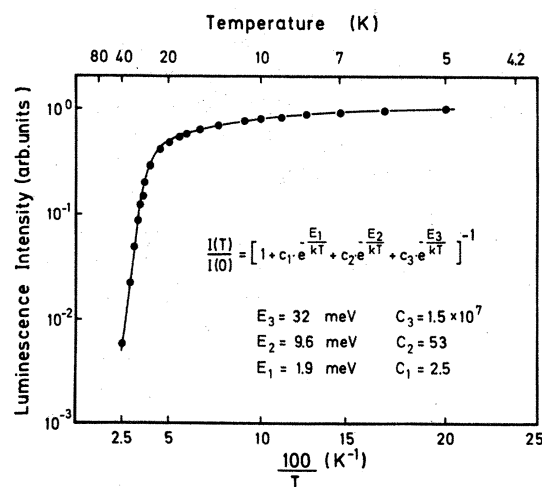


FIG. 6. Temperature dependence of the Cu_0^0 -line intensity. Points are experimental, diameters represent errors. A least-squares fit (full line) was performed using the inserted expression which refers to a four-level electronic system. Fit parameters are listed below.

$C_1 = g_1/g_0$ is the ratio of the degeneracies of the levels E_1 and E_0 , and the definition of C_2 and C_3 follows *mutatis mutandis* (with the necessary changes having been made). The values from the fit, $C_1 = 2.5$ and $C_2 = 53$, should therefore equal the numbers given above in this section. Actually, there is a large discrepancy between the two sets of values. Such discrepancies are familiar from other exciton systems¹⁸ although an explanation has not yet been given. As a striking result, we obtain a remarkably large value of C_3 suggesting that the coordinated level is a band; population of that level would then be equivalent to the ionization of the present system. The ionization energy from the exciton ground state is $E_{th} = E_3 = 32$ meV. We note for further discussion in Sec. VII that there is a vast difference of this value to the spectroscopic localization energy of the exciton which amounts to $\Delta E_{loc,X} = 140.3$ meV with respect to the free-exciton edge, or to $\Delta E_{loc,E_g} = 155.0$ meV with respect to the conduction-band edge using the accepted free-exciton binding energy of $E_X = 14.7$ meV in silicon.

V. UNIAXIAL STRESS SPLITTING OF THE COPPER LINES

Uniaxial stress reduces the symmetry of the crystal and may lift the degeneracy of the levels except for a remaining Kramers degeneracy. We have to distinguish between electronic and orientational degeneracies. Splitting effects due to the lifting of the orientational degeneracy have been studied by Kaplyanskii¹⁹ for noncubic centers in cubic crystals. It is generally assumed that for deep centers the splitting of a line due to electronic degeneracy effects is negligible. This assumption

was also made in the work of Kaplyanskii. In fact, the tendency of a reduction of the deformation potentials is experimentally well known even for the series of effective-mass-theory (EMT)-like shallow donors in silicon when the chemical shift increases.²⁰

In just one special case, the combined splittings due to both types of degeneracies were considered: Morgan and Morgan²¹ studied the uniaxial stress splitting of an exciton bound to an axially symmetric defect. The work was restricted to a $\langle 111 \rangle$ configuration and to an isoelectronic trap as binding center. These calculations have an experimental counterpart in the A, B, C isoelectronic line system in silicon where the experimental line splittings²² agree nicely with theory.²¹ In the present study, we observe a similar splitting of the copper NP Cu_0^0 line and show that it can be ascribed to an exciton bound to an isoelectronic copper pair in a—virtually— $J = 2$ state. The optical transition from this state becomes dipole allowed by the weak disturbing effect of the axial field.

The stress induced splitting of the Cu_0^0 line is shown in Fig. 7. We distinguish two stress regimes. For low stress, up to approximately 10 MPa, two line components split anisotropically apart for stress along $\langle 111 \rangle$ and $\langle 110 \rangle$, respectively, and one unsplit line is observed for stress along $\langle 100 \rangle$. We interpret these spectra as due to an axial center with $\langle 111 \rangle$ symmetry axis where stress lifts only the orientational degeneracy. For trigonal symmetry, all centers orientated along different $\langle 111 \rangle$ directions remain equivalent because they are subjected to the same “effective” strain when stress is applied along $\langle 100 \rangle$. Therefore, no splitting can occur. For stress along $\langle 111 \rangle$ and $\langle 110 \rangle$, theory predicts twofold splittings from the piezospectroscopic tensor¹⁹ as are actually observed.

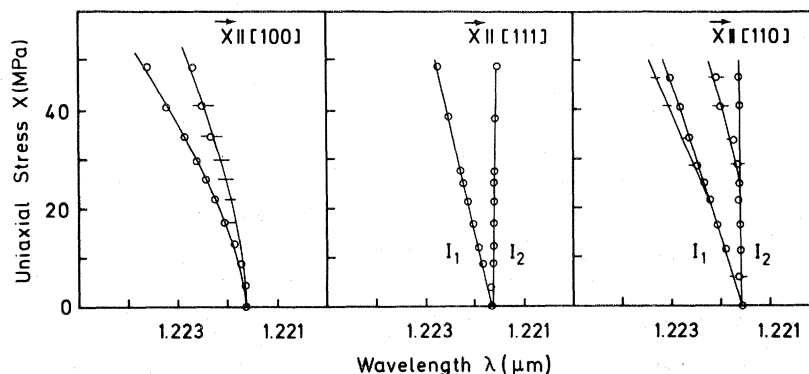


FIG. 7. Splitting of the Cu_0^0 line for uniaxial stress \vec{X} along the main crystallographic directions.

These linear splittings are superimposed by the effects of the lifting of the electronic degeneracy at stress higher than about 10 MPa. The overall splittings are consistent with the Morgan-Morgan model when we assume that the hole splitting which originates from the internal strain along the copper-pair axis is small compared to the electrostatic electron-hole interaction, and is contained in the halfwidth of the Cu_0^0 line at zero stress. In terms of the Morgan-Morgan model, the present trap is close to the "spherical" limit of the exciton (cf. Fig. 1 in Ref. 21). The electronic effects are further responsible for the nonlinear portions of the observed line shifts. A quantitative discussion of the data on the basis of the theory will be given elsewhere. At the moment, we shall concentrate on the thermalization properties and the relative polarizations of the two line components I_1 and I_2 which show up for stress along $\langle 111 \rangle$ (Fig. 8). Since, according to Fig. 7, the spacing between I_1 and I_2 is proportional to the stress applied, the intensity ratio of I_2 to I_1 in Fig. 8 (upper part) corresponds to a Boltzmann function. The activation energy is about 0.02 meV/MPa which is practically identical with the spectroscopic spacing of the lines (0.82 meV/40 MPa). We extrapolate the experimental points back to zero stress and find an intensity ratio of $I_2/I_1=3$. This is just the ratio of the statistical weights of a trigonal center being with equal probability orientated along the one $\langle 111 \rangle$ direction which is parallel to the stress, or along the three other $\langle 111 \rangle$ -type directions which remain equivalent under the stress. Thermalization

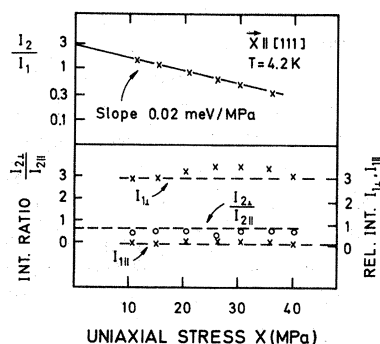


FIG. 8. Upper part denotes intensity ratio of the stress-split components I_1 and I_2 for $\vec{X} \parallel [111]$. The theoretical value is $I_2/I_1=3$ for a trigonal center and an optical σ oscillator without alignment under stress. Lower part denotes intensity ratio of the polarized components, $I_{21}/I_{2||}$ and relative intensity values of the polarized components $I_{1||}$ and $I_{2||}$. Theoretical values (dotted lines) are $I_{21}/I_{2||}=5/8$, and $I_{1||}/I_{2||}=3/0$.

of the line components then simply means that all centers in the crystal align along the stress axis because this orientation is energetically favored. We note from the completeness of thermalization which we observed in all experiments irrespective of the time left for reorientation that this process is evidently accomplished rapidly. This may point to a model where at least one copper atom of the pair is located on an interstitial site from where it can rapidly move to other interstitial sites of equivalent pair configuration.

We find also consistency of our assumed trigonal trap with the observed polarizations of the I_1 and I_2 line components (Fig. 8, lower part) when we suppose that the oscillator corresponding to the optical transition is σ -type connecting electronic states of different angular momenta. The ratio of the polarized I_2 line components, $I_{21}/I_{2||}$, is found to be stress independent and to have an experimental value of about 0.55. This is in fairly close agreement with the theoretical value of 0.625 valid for a trigonal center according to Kaplyanskii. For the I_1 line, we give in Fig. 8 the relative intensities of the polarized components instead of the ratio since I_1 is practically zero over the entire stress range. The theoretical intensities which correspond to the statistical weights of the respective oscillators are compared in Fig. 8 and show also a satisfactory agreement with experiment.

For $\langle 100 \rangle$ stress, the observed polarizations of the line components do not change at small stress values but exhibit slight changes at higher stress values which are in agreement with the theoretical considerations of Morgan and Morgan.²¹ An analysis is more difficult for stress along $\langle 110 \rangle$ due to the fourfold splitting, but leads also to a fair agreement with the theory. The polarization features for all stress directions sum up to support the model of a σ oscillator at a trigonal center.

All phonon satellites exhibit splittings identical with that of the NP line. Only at high stress values, we find small deviations from this behavior. For example, for $\langle 110 \rangle$ stress at 100 MPa, the centers which are orientated perpendicular to the stress axis show no change in phonon energy whereas those which are orientated along the stress axis exhibit increased displacement energies of 7.5 meV.

VI. ZEEMAN SPLITTING OF THE COPPER LINES

The splitting of the Cu_0^0 line was studied in magnetic fields up to 5.3 T. No Zeeman spectra could

be recorded of other lines because their halfwidths are too large so that splittings only show up as line broadenings. The Cu_0^0 -line Zeeman spectra for fields along the main crystallographic directions are shown in Fig. 9.

We observe for $\vec{H}||[100]$ five components which are not fully resolved in Fig. 9 but can be clearly separated by polarized measurements. One unresolved component, e.g., is located on the high-energy shoulder of the strongest low-energy Zeeman line. A further component is hidden below the high-energy side of the broader central Zeeman line. For fields along the other two directions we observe more than five components. We explain the extra components in excess of five as due to the axial nature of the copper defect consistent with the $\langle 111 \rangle$ trigonal symmetry classification from the stress data. For each direction, all Zeeman components thermalize with the low-energy component so that the splittings occur entirely in the transition initial state. Taking the simple case of the $\langle 100 \rangle$ direction free from orientational anisotropy effects, we conclude that we are concerned with a quintuplet-to-singlet Zeeman spectrum.

We take up again in Fig. 10 our interpretation in terms of an isoelectronic axial copper center which was anticipated in Sec. II. The Cu_0^0 -line upper

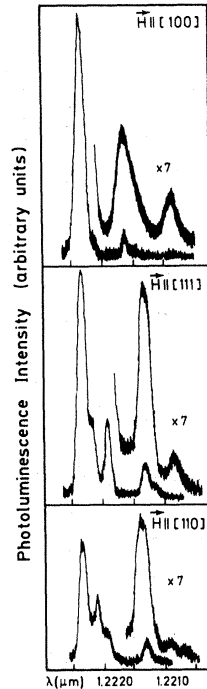


FIG. 9. Zeeman splitting of the Cu_0^0 line for a magnetic field H of 5.3 T along the main crystallographic directions.

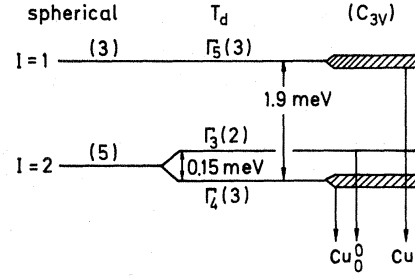


FIG. 10. Level scheme of the exciton and recombination transitions to the isoelectronic ground state. Possible, unresolved splittings of the levels under a uniaxial (internal) strain along $\langle 111 \rangle$ correspond to C_{3v} symmetry and are schematically shown by hatched areas. Numbers in parentheses are degeneracies.

ground state corresponds, in a spherical approximation, to the angular momentum $J=2$ of an exciton bound to the isoelectronic trap. The j - j electrostatic interaction of the hole and the electron splits the $J=1$ state apart from $J=2$ by 1.9 meV, and the excitonic decay from $J=1$ to the crystal ground state $J=0$ is the origin of the Cu_1^0 line. The effect of the internal built-in strain from the atomic copper dumbbell is so small that the associated splittings are almost contained in the half-width of the Cu_0^0 line, and can be ignored against the j - j electrostatic interaction. We recall that in Fig. 2 the Cu_0^0 line exhibits an unresolved high-energy shoulder which thermalizes with the Cu_0^0 line and is displaced by about 0.15 meV. Whereas at first sight it is not obvious whether this splitting results from the internal axial strain or from a cubic crystal-field splitting of the $J=2$ level, we shall analyze the Zeeman data in terms of a T_d crystal-field effect using a simple cubic model.

We refer to Merz *et al.*²³ who studied excitons bound to isoelectronic nitrogen in GaP. From group theory, they derived the interaction matrix which applies to the most general linear Zeeman interaction of exciton states with symmetry Γ_5 ($J=1$) and $\Gamma_3 + \Gamma_4$ ($J=2$) in T_d . One needs five independent parameters to describe the linear Zeeman splitting, $\gamma_1, \gamma_2, \gamma_3$, and δ_1, δ_2 : δ_1 gives the low-field splitting of the Γ_5 state; γ_2 and γ_3 give the splittings in the $(\Gamma_3 + \Gamma_4)$ manifolds; δ_1 and δ_2 mix the Γ_4 and Γ_5 , or Γ_3 and Γ_5 states, respectively, and cause nonlinear splittings at higher fields. We have numerically diagonalized the 8×8 interaction matrix and have fitted the results to the measured field dependence of the Cu_0^0 -line splitting (Fig. 11). The set of parameters given in Fig. 11 leads to a satisfactory fit for $\vec{H}||[100]$ but is less

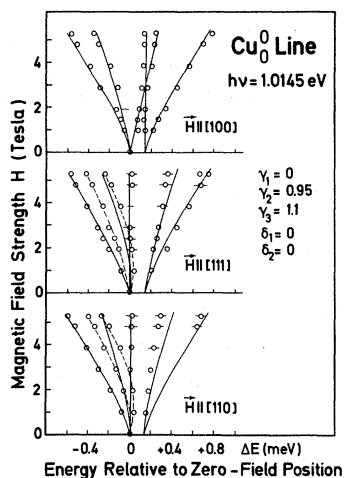


FIG. 11. Zeeman splitting of the Cu_0^0 line (circles) and fits using the inset numbers (full lines, see text). The fit comprises all lines for $\vec{H} \parallel [100]$, but neglects the extra Zeeman components which are observed for $\vec{H} \parallel [111]$ and $\vec{H} \parallel [110]$ due to the lifting of the orientational degeneracy of the binding center.

good for the other two directions. It turned out that another set exists which fits the $\langle 111 \rangle$ and $\langle 110 \rangle$ directions well but is in this case not too good for $\langle 100 \rangle$. This latter set has the same values of γ_1 , γ_2 , and γ_3 as before and values of δ_1 and δ_2 larger than all γ values. Since δ_1 and δ_2 describe the mixing of states from the $J=1$ with those from the $J=2$ manifolds whose electrostatic splitting is much larger than the low-field-induced splittings we would not ascribe too much physical significance to such large δ values. On the other hand, as long as δ_1 and δ_2 are small, their influence on the line positions is weak, and as a consequence, also variations of γ_1 do not largely alter the splittings. Unfortunately, we have no experimental splitting of the upper Γ_5 state on hand which would greatly help to determine γ_1 conclusively. Therefore, the value of γ_1 may not be regarded as too reliable. On the whole, we do not find a set of parameters which gives an overall fit to the experimental data better than the one shown in Fig. 11. There are more reasons why the fits should be regarded more or less qualitative. We have, e.g., neglected that the orientational degeneracy is lifted giving rise to the extra lines mentioned earlier. Also, diamagnetic shifts of lines are completely ignored. Therefore, we lay emphasis on the qualitative agreement between the Zeeman data and the theory used. In particular, we note that the lower-energy Γ_4 state splits threefold, and the higher-energy Γ_3 state splits twofold consistent

with the labeling chosen. The previously mentioned zero-field splitting of the Cu_0^0 line by 0.15 meV is also easily subsumed in the present analysis, and is in this interpretation due to the crystal field. Summing up these results we find evidence for our model of an exciton at an isoelectronic copper trap.

VII. MODEL DISCUSSION OF THE 1.014-eV COPPER EMISSION

In the previous sections, we have shown that the 1.014-eV emission originates from a copper pair in a $\langle 111 \rangle$ configuration. Copper was identified by the isotope effects due to ^{63}Cu and ^{65}Cu . Formation of a pair was concluded from the quadratic dependence of the luminescence intensity on the copper concentration, and the unimportance of shallow donors or acceptors and of contaminants for the radiation led us to discard a complex center consisting of more than two copper atoms. The luminescent system could be described in terms of an exciton bound to a copper trap of isoelectronic nature in $\Gamma_3 + \Gamma_4$ ($J=2$) or Γ_5 ($J=1$) states as is common for many isoelectronic systems.

We are now concerned with the question whether the copper atoms occupy both substitutional sites or both (T_d) interstitial sites or substitutional-interstitial sites. The first possibility is excluded since it seems unlikely that in this model the molecular dumbbell could easily align along the external uniaxial stress as was observed and described in Sec. V. This model is also in disagreement with the small size of the observed dissociation energy of the center, since relatively low temperatures from 150°C on are sufficient to destroy the center, as was observed in annealing experiments. There are two remaining possibilities both of which would allow for rapid reorientation under external stress since copper in an interstitial position is highly mobile even at very low temperatures. We cannot further distinguish between these alternatives from the present experiments.

At the end of Sec. IV, the striking difference between the thermal ionization energy (32 meV) and the spectroscopic localization energy (155.0 meV) of the exciton system was emphasized. Disagreements of energies as determined from the two methods are familiar for a number of isoelectronic systems (see Ref. 11, P. J. Dean), but in no case is the discrepancy so large as in our copper system and is the localization energy so high amounting to

$\sim 15\%$ of the band gap. We therefore conclude that we are concerned with an exciton which can be well described by the conception of an isoelectronic donor or acceptor.²⁴ Whereas it cannot be decided from the present experiments which of the two cases applies we correlate recent DLTS data with our data and suggest that the exciton corresponds to an isoelectronic donor. The donor electron is bound by 32 meV, close to the effective-mass binding energy ($E_d \approx 31$ meV) in silicon, and the hole representing the charge of the donor core is deeply bound by $E_h = 123$ meV in the short-range potential of the isoelectronic trap.

The hole binding of 123 meV as obtained in the isoelectronic donor model is not too different from a deep donor level which was recently observed in copper-doped silicon at $E_v + 0.102$ eV by the DLTS technique by Graff and Pieper⁵ and independently by Wünnel.²⁵ In DLTS, a single donor state ($0/+$) is associated with a charge transfer from the neutral defect state to a positively charged state when the position of the Fermi level moves towards the valence band. The above-mentioned DLTS level is, therefore, related with a hole binding of 0.102 meV. It is only observed in samples which were rapidly quenched after the diffusion of copper. This sample treatment corresponds to our procedure in preparing the silicon samples for the optical experiment, and could explain that other Cu-related levels do not agree with the presently discussed ones. Other levels were observed in Hall, photoconductivity and DLTS measurements at energies $E_c - 0.24$ eV (donor) and $E_v + 0.49$ eV (acceptor) by Collins and Carlson,² $E_v + 0.52$ eV, $+0.37$ eV, and $+0.24$ eV by Milnes,²⁶ and $E_v + 0.22$ eV and $+0.41$ eV by Kimerling *et al.*²⁷ Returning to the tentatively related optical and electrical values of $E_h = 123$ meV and $E_v + 0.102$ eV, respectively, one has to keep in mind that our thermal ionization energy of the electron, 32 meV, may be uncertain by about ± 2 meV, and that in particular the uncertainty of the DLTS level may amount to the order of 10 meV.

We believe that the approximate coincidence of trap levels from DLTS and from optical data may not be accidental. There are other systems in silicon where we recognize similar tendencies after appropriate evaluation of our luminescence measurements. Iron-related defects (the exact structure of the defects is not yet known) have been shown to emit a sharp line series with a no-phonon transition at $h\nu = 0.7343$ eV.⁷ The thermal ionization energy of the no-phonon line was found to be

$E_{th} = 31$ meV from which a residual one-particle binding energy of $E_t = 404$ meV results. This value is in excellent agreement with the donor level $E_v + 400$ meV of Wünnel and Wagner²⁸ in iron-doped silicon. As another example we mention the case of luminescence lines in silicon which we attribute to Cr-B pairs.⁹ In this case, the no-phonon line is positioned at $h\nu = 0.8455$ eV with a thermal ionization energy of $E_{th} \sim 15$ meV from which we obtain $E_t = 309$ meV. DLTS measurements, on the other hand, have yielded a trap level of $E_v + 290$ meV for Cr-B pairs,⁵ again in fair agreement with our value for E_t .

VIII. SUMMARY

Intense luminescence lines characteristic of copper-doped silicon samples have been studied. The samples were prepared by diffusion of evaporated copper films, and by rapid quenching of the samples to room temperature. The luminescence spectra exhibit features common of other transition-metal impurities in silicon. In particular, a series of low-energy satellites can be identified as phonon replicas of the principle no-phonon emission associated with local vibrations of the binding center. The characteristic local-mode phonon energy is 7.0 meV. The defect is formed by two copper atoms; this is deduced from the observed isotope shifts of ⁶³Cu and ⁶⁵Cu, and from reaction kinetics. The symmetry-dependent properties can be described as being due to an exciton localized at an isoelectronic copper trap with trigonal axial symmetry. The axial component of the bound exciton is only weak, and an approximate description in terms of cubic ($\Gamma_3 + \Gamma_4$) and (Γ_5) states is possible. Considerable differences between the thermal activation energy and the spectroscopic localization energy indicate that the exciton corresponds to an isoelectronic donor. It is suggested that a correlation exists between the primary hole binding to the isoelectronic trap and recently observed DLTS levels in quenched, copper-doped silicon.

ACKNOWLEDGMENTS

We would like to express our gratitude to A. Axmann [Institut für Angewandte Festkörperforschung, (IAF), Freiburg] for the implantation of

the copper isotopes. We thank also P. Wagner (Heliotronic, Burghausen) and H. Conzelmann (Universität Stuttgart) for many helpful discussions, and M. H. Pilkuhn for the excellent experi-

mental facilities which enabled this work. The support of the Bundesministerium für Forschung und Technologie (BMFT) under Contract No. NT 2555/9 is gratefully acknowledged.

- ¹J. D. Struthers, J. Appl. Phys. **27**, 1560 (1956).
- ²C. B. Collins and R. O. Carlson, Phys. Rev. **108**, 1409 (1957).
- ³F. A. Trumbore, The Bell System Technical Journal, January 1960, p. 205.
- ⁴R. N. Hall and J. H. Racette, J. Appl. Phys. **35**, 379 (1964).
- ⁵K. Graff and H. Pieper, in *Semiconductor Silicon 1981, Proceedings of the 4th International Symposium on Silicon Materials Science and Technology*, edited by H. R. Huff and R. J. Kriegler (The Electrochemical Society, Pennington, New Jersey, 1981), Vol. 81-5, p. 331.
- ⁶G. W. Ludwig and H. H. Woodbury, in *Solid State Physics*, edited by F. Seitz and D. Turnbull (Academic Press, New York, 1962), Vol. 13.
- ⁷J. Weber and P. Wagner, J. Phys. Soc. Jpn. **49**, Suppl. A, 263 (1980).
- ⁸J. Weber, R. Sauer, and P. Wagner, J. Lumin. **24-25**, 155 (1981); and unpublished.
- ⁹J. Weber *et al.* (unpublished).
- ¹⁰J. Mazzaschi, J. C. Brabant, Mme. B. Brousseau, J. Barrau, M. Brousseau, F. Voillot, and P. Bacuvier, Solid State Commun. **39**, 1091 (1981).
- ¹¹P. J. Dean, J. Lumin. **7**, 51 (1973); B. Monemar, *ibid.* **5**, 239 (1972); P. J. Dean, D. J. Robbins, S. G. Bishop, J. A. Savage, and P. Porteous, J. Phys. C **14**, 2847 (1981); E. F. Gross, V. I. Safarov, V. E. Sedov, and V. A. Marushak, Fiz. Tverd. Tela (Leningrad) **11**, 348 (1979) [Sov. Phys.—Solid State **11**, 277] (1969); F. Willmann, D. Bimberg, and M. Blätte, Phys. Rev. B **7**, 2473 (1973).
- ¹²J. Weber, W. Schmid, and R. Sauer, Phys. Rev. B **21**, 2401 (1980).
- ¹³G. S. Mitchard, S. A. Lyon, K. R. Elliott, and T. C. McGill, Solid State Commun. **29**, 425 (1979); M. L. W. Thewalt, U. O. Ziemelis, and R. R. Parsons, *ibid.* **39**, 27 (1981).
- ¹⁴N. S. Minaev, A. V. Mudryi, and V. D. Tkachev, Fiz. Tekh. Poluprovodn. **13**, 395 (1979) [Sov. Phys.—Semicond. **13**, 233 (1979)].
- ¹⁵V. Heine and C. H. Henry, Phys. Rev. B **11**, 3795 (1975).
- ¹⁶J. A. van Vechten, Phys. Rev. B **13**, 946 (1976).
- ¹⁷F. E. Williams and H. J. Eyring, J. Chem. Phys. **15**, 289 (1947).
- ¹⁸D. Bimberg, M. Sondergeld, and E. Grobe, Phys. Rev. B **4**, 3451 (1971).
- ¹⁹A. A. Kaplyanskii, Opt. Spectrosc. (USSR) **16**, 329 (1964); J. Phys. (Paris) **28**, 4 (1967).
- ²⁰See, e.g., V. J. Tekippe, H. R. Chandrasekhar, P. Fischer, and A. K. Ramdas, Phys. Rev. B **6**, 2348 (1972).
- ²¹J. v. W. Morgan and T. N. Morgan, Phys. Rev. B **1**, 739 (1970).
- ²²J. Weber and R. Sauer (unpublished).
- ²³J. L. Merz, R. A. Faulkner, and P. J. Dean, Phys. Rev. **188**, 1228 (1969).
- ²⁴J. Hopfield, D. G. Thomas, and R. T. Lynch, Phys. Rev. Lett. **17**, 312 (1966).
- ²⁵K. Wünnel, Max-Planck-Institut für Festkörperforschung, Stuttgart (private communication).
- ²⁶A. G. Milnes, *Deep Impurities in Semiconductors* (Wiley, New York, 1973).
- ²⁷L. C. Kimerling, J. L. Benton, and J. J. Rubin, in *Defects and Radiation Effects in Semiconductors 1980*, edited by R. R. Hasiguti (Institute of Physics, Bristol, 1981), p. 217.
- ²⁸K. Wünnel and P. Wagner, Solid State Commun. **40**, 797 (1981). These authors discuss that some properties of their 0.4-eV level disagree with other 0.4-eV DLTS levels reported in literature. Their level has a similar annealing behavior to our luminescent defect.